DESIGN PARAMETERS FOR AN ORBITING TOPSIDE SOUNDER FOR MARS AND VENUS AND SOME COMPARISONS WITH THE ORBITING OCCULTATION EXPERIMENT

July 30, 1968

Bellcomm, Inc.

DESIGN PARAMETERS FOR AN ORBITING TOPSIDE SOUNDER FOR MARS AND VENUS AND SOME COMPARISONS WITH THE ORBITING OCCULTATION EXPERIMENT

July 30, 1968

W. R. Sill

Work performed for Manned Space Flight, National Aeronautics and Space Administration under Contract NASW-417.

ABSTRACT

The design parameters for a Venus and Mars topside sounder are discussed and compared to tnose for the earth orbiting Alouette topside sounders. In the three areas of frequency range, range (time) resolution and power requirements, improvements of the Alouette systems are required.

In order to probe the low densities on the Martian night side and the low densities in the solar wind-ionosphere interaction region, an extension to frequencies lower than those used on Alouette II (.2 MHz) would be required. Extending the measurements to such low frequencies presents certain problems since the wavelengths involved ($>10^3$m) require long antennas.

The largest factor affecting the power requirement is the spatial attenuation (spreading) of the wave energy. Also of importance is the electron collisional absorption loss, which for the model ionospheres of Mars and Venus is greater than that for the topside earth ionosphere.

The small scale heights near the ionosphere peaks of Mars (25 km) and Venus (13 km) would require some improvement in range resolution over that of the Alouette satellites, which have a resolution of the order of 10 km. This also leads to an increase in the power requirement since increasing the range resolution requires opening the receiver bandwidth with a resultant increase in the cosmic noise background.

The occultation experiment when compared to a topside sounder has the advantage of fewer and higher frequencies (>10 MHz), which utilize smaller antennas, the capability of measuring very low electron densities (5 cm^{-3}), and bottomside as well as topside measurements. Some of the disadvantages of the occultation experiment are the lateral averaging along the ray path of the ionospheric properties and the long time needed to provide information on the local time (solar zenith angle) dependence of the ionosphere.

TABLE OF CONTENTS

DESIGN PARAMETERS FOR AN ORBITING TOPSIDE SOUNDER FOR MARS AND VENUS AND SOME COMPARISONS WITH THE ORBITING OCCULTATION EXPERIMENT

1.0 INTRODUCTION

One of the most useful devices for the study of the earth's ionosphere is the ionosonde. The typical ionosonde consists of a pulsed, variable frequency transmitter and a receiver which is used to measure the time delay of the reflected pulses. With a ground based sounder the wave pulses are transmitted vertically up toward the underside of the ionosphere, which consists of several regions of successively increasing electron density. These regions are the D region (60 to 90 km, electron density - $N_e \sim 10^3$ cm^{-3}), the E region (90 to 140 km, $N_e \sim 10^5$ cm^{-3}), the F_1 region (140 to 200 km, $N_e \sim 5 \times 10^5$ cm^{-3}) and the F_2 region (greater than 200 km, $N_e(\max) \sim 10^6$ cm^{-3} at 350 km decreasing to 10^4 cm^{-3} at 10^3 km). The transmitted pulses will be reflected from that part of the ionosphere where the wave frequency of the pulse is equal to the plasma frequency. The plasma frequency is proportional to the square root of the electron density (Equation 1) so that the measurement of the time delay (τ) as a function of frequency gives a profile of electron density as a function of virtual range, $h'(f) = c\tau(f)/2$ (see Appendix A, Equation A.7). These curves of electron density (or plasma frequency) vs. virtual range are called ionograms and various techniques exist for converting the data contained in an ionogram into an electron density profile in terms of the true range (or altitude).

The pulses with a low wave frequency ($\sim$1 MHz) are reflected from the low density, low altitude regions, and as the wave frequency increases the reflection point moves up into the denser regions. When the wave frequency exceeds the maximum F_2 plasma frequency ($\sim$10 MHz) the waves will not be reflected but will continue to propagate out into space. For this reason, the ground based ionosonde can probe only that part of the ionosphere below the F_2 peak ($\sim$350 km).

In order to explore the region above the F_2 peak, various other ground based methods were developed such as the incoherent backscatter technique. With the advent of the

space age, it became possible to probe the topside ionosphere above the F_2 peak by placing an ionosonde on an earth orbiting satellite. The orbiting sounder has proved to be an invaluable tool for the study of the topside ionosphere. For example, the first of these topside sounders, Alouette I, made more than a quarter of a million ionograms which provided data on the electron density between the satellite orbit (10^3 km) and the F_2 peak.

The only other planetary ionospheres about which we have any direct knowledge are those of Mars and Venus. The ionospheres of these planets were detected by the radio occultation experiments of Mariners 4 and 5[1,2,3]. In the occultation experiment the Doppler shift of a signal passing through the ionosphere is measured (Figure 1).

On future missions, it may be possible to use either orbiting occultation or orbiting topside sounding techniques for the continuing study of these planetary ionospheres. The purpose of this note is to investigate some of the specifications for Mars and Venus topside sounders and to compare the relative merits of orbiting topside sounders and orbiting occultation devices.

2.0 DESIGN PARAMETERS FOR A TOPSIDE SOUNDER

Three of the more important design parameters for a topside sounder are 1) the frequency range of the transmitter and receiver, 2) the time resolution required in measurement of the reflected pulses and 3) the power requirements of the transmitter.

2.1 Frequency Ranges and Antennas

The frequency range is dictated by the range of electron densities that are to be detected. The equation relating the electron density to the plasma frequency (f_p) is

$$f_p = 9 \times 10^3 \sqrt{N_e} \qquad (1)$$

where N_e = number of electrons/cm^3.

For Venus a frequency range of .3 to 9.0 MHz, corresponding to electron densities from 10^3 to 10^6 cm^{-3}, would permit the

exploration of most of the day and night topside ionosphere below 500 km. The above frequency range corresponds to wavelengths from 33 to 1000 m. The long wavelengths associated with the lower frequencies would present problems in the design of antennas. The Alouette I topside sounder[4] made use of two antennas of 46 and 23 m length in order to cover the frequency range from .5 to 12 MHz (electron densities from 3×10^3 to 1.4×10^6 cm^{-3}). Alouette II uses two antennas of 22 and 72 meters to cover the band from .2 to 14 MHz (electron densities from 4×10^2 to 2×10^6 cm^{-3}).

A frequency range of .3 to 4 MHz would probably be adequate for the dayside ionosphere of Mars. However, the low densities expected on the night side (below 10^3 cm^{-3}) may require frequencies even lower than those of Alouette II.

2.2 Time and Range Resolution

The pulse length of 100 μsec used on Alouette provides a minimum time resolution of 100 μsec which corresponds to virtual range resolution of 30 km. For a large signal-to-noise ratio, better resolution is attainable and it is primarily limited by the rise time of the leading edge of the received pulse. The rise time response can be shortened by increasing the bandwidth of the receiver; however, opening the bandwidth increases the noise power (see next section). The receiver bandwidth on Alouette is 30 KHz, corresponding to a rise time of about 10 μsec and a range resolution of 3 km. The actual virtual range resolution on Alouette is probably somewhere between 3 and 10 km. This resolution is adequate for the earth (scale height ∿100 km), but the scale heights just above the ionospheric peaks of Mars (25 km) and Venus (13 km) are of the order of the above resolution, so that an improvement in resolution is probably required.

2.3 Power Requirements

The transmitted power is determined by the need to have the reflected pulse energy exceed the cosmic radio noise background. Along the propagation path the energy decreases due to geometrical spreading and collisional absorption. Other losses such as those due to antenna mismatch and polarization will be included but will not be discussed in detail.[4]

The effective Black Body temperature of the cosmic noise above 1 MHz is[4]

$$T = 5 \times 10^{7} f^{-2}_{MHZ} \ (^{\circ}K)$$

The cosmic noise power (P_{CN}) in a small band ($\Delta f_{MHz} << f_{MHz}$) is then

$$P_{CN} = KT\Delta f = 7 \times 10^{-10} \ \Delta f_{MHz}/f^{2}_{MHz} (\text{watts}) \qquad (2)$$

where K is Boltzmann's constant.

A desirable signal-to-noise ratio would be 10 so that the power of the received signal (P_r) should be

$$P_r = 10 \ P_{CN} = 7 \times 10^{-9} \Delta f/f^{2} \qquad (3)$$

The geometrical spreading of the signal reduces the power flux (p) in accordance with the inverse of the distance squared.

$$p = P_T/4\pi(2r)^{2} \ (\text{watts}/m^{2}) \qquad (4)$$

where

r = distance to the (plane) reflecting layer in meters (r is a function of frequency)

The effective area of an isotropic antenna is proportional to the square of the wavelength of the signal so that the received signal is

$$P_r = \frac{P_T \lambda^{2}}{(8\pi r)^{2}} = \frac{1.42 \times 10^{2} \ P_T}{r^{2} f^{2}_{MHz}} \ (\text{watts}) \qquad (5)$$

The ratio of the received to the transmitted power is shown as a function of frequency and range in Figure 2. The superimposed dashed curves show the range vs. frequency results for the model daytime ionospheres of Mars and Venus (Appendix C). The maximum spatial attenuation (at the highest frequency) is -100 db for Mars and -110 db for Venus. The path length for both cases is about 400 km (satellite orbit at 500 km). For the night models the lower frequencies (lower electron densities result in lower plasma frequencies) lead to smaller spatial attenuation.

Combining Equations 3 and 5 the required transmitted power is

$$P_T = \text{Const. } r(f)^2 \, \Delta f_{MHz} \qquad (6)$$

Equation 6 shows that the decrease in the cosmic noise power with frequency is balanced by the decrease in effective cross section of the antenna so that the required transmitter power depends only on the range and the bandwidth. As the range distance to the reflection point in the ionosphere increases with frequency, the greatest power is required for the highest frequency.

In the derivation of Equation 6 we have considered only spatial attenuation and the cosmic noise. Other sources of attenuation such as collisional absorption, antenna mismatch and polarization losses have been neglected. The latter two losses plus some others have been estimated for Alouette I at -22 db and they can be expected to be of a similar magnitude for any similar topside sounder.

The final loss to be considered is that due to the electron collisional absorption of the sounding waves. These losses have been calculated in Appendix C for model ionospheres of Mars and Venus, and in general they are found to increase with increasing frequency. For Venus the dayside E and F_1 models have a maximum absorption of -13 db at 9 MHz. The lower electron densities on the Venus night side lead to maximum attenuation of only -5 db. The Martian models have maxima of -8 db and -70 db at 3 MHz for the F_2 and E models, respectively. These are to be compared with a maximum of -5 db at 9 MHz for an earth F_2 topside ionosphere.

The various losses, cosmic noise, and the required transmitted power are given in Tables 1 and 2. The cosmic noise power was calculated from Equation 2 using a bandwidth of 30 KHz. The signal-to-noise ratio was taken to be 10. The spatial attenuation was calculated from Equation 5 and the range values were based on the ionograms of Appendix C (satellite orbit at 500 km). The above numbers for bandwidth, signal-to-noise ratio and spatial attenuation are meant to be representative. Variations of the above parameters as they affect the transmitted power can easily be determined from the tables and the previous equations.

For example, as was mentioned earlier an increase in range resolution would be desirable. Increasing the range resolution by a factor of 2 would require doubling the bandwidth. This would lead to an increase in the cosmic noise and the transmitted power by a factor of 2.

The signal-to-noise ratio was assumed to be 10; however, visual integration is capable of providing a gain of about 6 db[4]. This is equivalent to reducing the signal-to-noise ratio by a factor of 4. In this case the required power is 1/4 that given in the tables. The spatial attenuation is calculated for an orbit of 500 km (maximum range 400 km), and increasing the orbit to 10^3 km would lead to a maximum range of about 900 km. Since the spatial attenuation is proportional to r^{-2} the power requirements would be increased by a factor of 5 (7 db). The collisional attenuation will not be greatly altered for the higher satellite orbit as most of the attenuation takes place in the low altitude region near the ionospheric peak.

For a Venus topside sounder the required transmitted power on the night and day sides is 130 and 820 watts, respectively (Table 1). The smaller power figure for the night side is a consequence of the lower collisional attenuation only, since the smaller spatial attenuation is countered by an increased cosmic noise.

The required daytime power is 8 times larger than that used on Alouette I (100 w) and almost 3 times that used on Alouette II (300 w). However, in the design of Alouette I allowance was made for the gain provided by visual integration. If a signal-to-noise ratio of 2.5 is adequate (visual integration) the maximum daytime power is reduced to 200 w. Increasing the range resolution or increasing the satellite orbit (increasing the range) would of course require an appropriate increase in transmitted power.

Table 2 lists the losses, cosmic noise and power requirements for the two daytime Martian models. The transmitted power for the F_2 model is 234 watts and for the E model it is 10^8 watts. The prohibitively large power required by the E model results from the very large (-70 db) collisional absorption losses. The E model is included as an example of how large the power requirements could be in an extreme case. Recently some workers have expressed the opinion that the main layer is most likely of the F_1 type. The neutral density near the peak in an F_1 layer could be as much as 2 orders of magnitude larger than in the F_2 model of Appendix B, but still less than the neutral density of the E model. Even with the larger neutral density of the F_1 model the collision frequency above the peak would be dominated by the electron-ion term, so that the calculated absorption would not be greatly different from that of the F_2 model. Thus either an F_2 or F_1 model for the main layer would result in acceptable collisional losses, but an E model would certainly lead to excessive power requirements.

If a signal-to-noise ratio of 2.5 is acceptable (visual integration), the power requirement for the F_2 model is reduced to 60 watts. Increasing the bandwidth by a factor of 2, for the purpose of improving the range resolution, or increasing the satellite orbit to 10^3 km (range 900 km) would still leave the power requirements within acceptable limits.

In summary, a topside sounder for Mars or Venus, when compared to Alouette, would require a somewhat lower frequency range, better time resolution and most likely higher transmitter power. Except for the very large power required by the Martian E model and the antenna size problems, which arise from the desire to measure densities below 10^2 cm^{-3}; most of the above requirements should be attainable with present technology.

3.0 DISCUSSION OF THE OCCULTATION AND TOPSIDE SOUNDER EXPERIMENTS AND CONCLUSIONS

One of the more important differences between occultation experiments and topside sounders is the frequency used in each device. The occultation radio waves must pass through the ionosphere and hence their frequency must be greater than the plasma frequency. On the other hand, the

topside sounder waves are reflected within the ionosphere and so their frequency must be less than the maximum plasma frequency. From the standpoint of antennas the occultation device is more attractive since the higher frequencies involved can employ smaller antennas. Another advantage of the occultation experiment is that bottomside measurements are possible since the frequencies are greater than the maximum plasma frequency.

In the dual frequency occultation experiment of Mariner 5, frequencies of 40 and 400 MHz were used to measure electron densities of the order of 10 to 10^4 cm^{-3}. This pair of frequencies turned out to be too sensitive to measure the higher densities and small scale heights in the lower daytime ionosphere of Venus. In this case the less sensitive S-band (2300 MHz) data was used to determine the electron densities in this region. Another pair of frequencies between 400 and 2300 MHz would have been able to probe the lower ionosphere more effectively. Thus an orbiting occultation device might use 4 to 6 frequencies between 10 and 10^4 MHz to investigate the electron density range from 10 to 10^6 cm^{-3}.

We might contrast these frequency requirements with those of the Alouette topside sounder. Alouette I makes approximately 10^3 measurements at 13 KHz intervals in the frequency range between .5 and 12 MHz. At these frequencies the separation of 13 KHz yields an electron density resolution of better than a few percent. Certainly a topside sounder can be constructed with fewer frequencies at a sacrifice of resolution in electron density. For example, 6 frequencies at .55, 1.0, 1.7, 3.3, 5.5 and 10 MHz will permit measurements at $3x10^3$, $1x10^4$, $3x10^4$, $1x10^5$, $3x10^5$ and 10^6 electrons/cm^3. With respect to low density measurements, a more recent satellite (Alouette II) has extended the low frequency range to .2 MHz corresponding to an electron density of $4x10^2$ cm^{-3}.

Considering the geometry of the measurement (Figure 1) one sees that the vertical probing of the topside sounder has the capability of measuring in detail the horizontal variations. A topside sounder with data storage can measure the local time (dependence on solar zenith angle) variations, including measurements made on the side away from earth. In contrast, the occultation measurement results in an averaging of the lateral variations and in addition the measurement is made only above the limbs of the planet. One must wait for a relatively long time before the earth-planet geometry changes sufficiently to provide the local time coverage.

The many advantages of the occultation measurement suggest that it would be preferable to a topside sounder for the next stage in the study of planetary ionospheres. These advantages are the small number of frequencies (4 to 6), higher frequencies and hence smaller antennas, the capability of measuring very low electron densities ($5\ cm^{-3}$), and bottomside as well as topside measurements. Two disadvantages are the lateral averaging along the ray path (see Figure 1) and the limited coverage, that is, it can probe only that portion of the ionosphere near the limbs.

One of the most interesting regions in the ionospheres of Mars and Venus is that portion which interacts with the solar wind. On the day side of Venus this occurs at an altitude of about 500 km where the density increases from interplanetary values ($\sim 5\ cm^{-3}$) to $10^4\ cm^{-3}$. Only the occultation measurement has the required sensitivity to allow the detailed study of all of this region. Perhaps this alone is sufficient reason for recommending the occultation experiment.

1014-WRS-jan

W. R. Sill

W. R. Sill

Attachments
Figures 1, 2,
B.1-B.6,
C.1-C.4

REFERENCES

1. Mariner Stanford Group, "Venus: Ionosphere and Atmosphere as measured by Dual-Frequency Radio Occultation of Mariner V," Science 158, p. 1678, 1967.

2. Kliore, A., et al., "Atmosphere and Ionosphere of Venus from the Mariner V S-Band Radio Occultation Measurement," Science 158, p. 1683, 1967.

3. Fjeldbo, G. and Eshleman, V. R., "The Atmosphere of Mars Analyzed by Integral Inversion of the Mariner IV Occultation Data," Radioscience Laboratory, Stanford Electronics Laboratory, SV-SEL-67-109, 1967.

4. Molozzi, A. R., "Instrumentation of the Ionospheric Sounder Contained in the Satellite 1962 Beta Alpha (Alouette)," in Space Research, Ed. P. Muller, North-Holland Publishing Co., 1964.

5. Hartz, T. R., "Spectrum of the Galactic Radio Emission between 1.5 and 10 Mcls as Observed from a Satellite," Nature 4941, p. 173, 1964.

6. Budden, K. G., Radio Waves in the Ionosphere, Cambridge University Press, 1961.

7. Fjeldbo, G., W. C. Fjeldbo and V. R. Eshleman, Journal of Geophysical Research, 71, p. 2307, 1966.

8. Chamberlain, J. W. and M. B. McElroy, "Martian Atmosphere: Mariner Occultation Experiment," Science 152, p. 21, 1966.

TABLE 1

POWER REQUIREMENTS FOR VENUS TOPSIDE SOUNDER,

ORBIT AT 500 KM.

E or F_1 MODEL

	Night - .9 MHz*	Day - 9 MHz*
	Losses	Losses
Spatial (400 km)	- 90 db	- 110 db
Collisional	- 5	- 13
Others	- 22	- 22
Total	- 117 db	- 145 db
P_r/P_T =	$10^{-11.7}$	$10^{-14.5}$
P_{CN}^{**} =	2.6×10^{-11} watts	2.6×10^{-13} watts
$P_r = 10\ P_{CN}$ =	2.6×10^{-10} watts	2.6×10^{-12} watts
P_T =	$\frac{2.6\times10^{-10}}{10^{-11.7}} = 130$ watts	$\frac{2.6\times10^{-12}}{10^{-14.5}} = 820$ watts

*Maximum collisional and spatial losses at these frequencies

**Noise in 30 KHz bandwidth

TABLE 2

POWER REQUIREMENTS FOR MARS TOPSIDE SOUNDER,

ORBIT AT 500 KM

DAYTIME IONOSPHERE*

	F_2 Model - 3 MHz**	E Model - 9 MHz**
	Losses	Losses
Spatial (400 km)	- 100 db	- 100 db
Collisional	- 8	- 70
Others	- 22	- 22
Total	- 130 db	- 192 db
P_r/P_T =	10^{-13}	$10^{-19.2}$
P_{CN}^{***} =	2.34×10^{-12} watts	2.34×10^{-12} watts
P_r =	$10\ P_{CN} = 2.34 \times 10^{-11}$ watts	2.34×10^{-11} watts
P_T =	$\frac{2.34 \times 10^{-11}}{10^{-3}} = 234$ watts	$\frac{2.34 \times 10^{-11}}{10^{-19.2}} = 3.7 \times 10^{8}$ watts

*Nighttime losses will be less than these

**Maximum spatial and collisional losses at these frequencies

***Noise in 30 KHz bandwidth

APPENDIX A

Wave Propagation in a Plasma

The index of refraction (n) in a plasma in the absence of a magnetic field is given by

$$n = \mu - i\chi = [1-X/(1-iZ)]^{1/2} \qquad A.1$$

where

μ = real part of index of refraction

χ = imaginary part of index of refraction

$X = \omega_p^2/\omega^2$

$Z = \nu_e/\omega$

ω_p = plasma frequency = $5.64\ 10^4\ N_e^{1/2}$

ν_e = total collision frequency = $\nu_{ei}+\nu_{en}$

ν_{ei} = electron-ion collision frequency

$$= [34.+4.2x\log (T_e^3/N_e)]\ N_e/T_e^{3/2} \qquad A.2$$

ν_{en} = electron-neutral collision frequency

$$= 5.4x10^{10}\ N_n T_e^{1/2}$$

N_e = electron number density (cm^{-3})

N_n = neutral number density (cm^{-3})

T_e = electron temperature (°K)

When the collision frequency is low ($Z<<1$) and the frequency is not close to the plasma frequency ($X\neq 1$), the components of index of refraction are approximately

$$\mu \simeq [1-X]^{1/2} \qquad A.4$$

$$\chi \simeq ZX/2\mu \qquad A.5$$

APPENDIX A

In the low collision frequency limit ($Z \sim 0$) a wave propagating into a plasma of increasing electron density (X increasing) will be reflected when X=1. At this point the wave frequency equals the plasma frequency and n=0. The details of this reflection process and those for the more complicated case when $Z \neq 0$ are treated in many texts (6).

A wave propagating through a plasma of slowly varying index will have its amplitude reduced by a factor

$$R = e^{-k_o \int_S \chi ds} \qquad \text{A.6}$$

χ = imaginary part of index of refraction

k_o = free space wave number

The group travel time (group delay) is given by the integral

$$\tau_g = \frac{1}{c} \int_S \mu_g ds = \frac{1}{c} \int_S \frac{ds}{\mu} \qquad \text{A.7}$$

where

c = velocity of light

μ_g = group refractive index = $1/\mu$ = 1/phase refractive index

In the case of a vertical sounding experiment the path S is taken from the transmitter to the reflection point. In this work it will be assumed that the reflection takes place at that point where the wave frequency is equal to the plasma frequency (X=1). Although the integrand in A.7 ($1/\mu$) blows up at the point of reflection ($\mu=0$) the integral remains finite.

The integrals in A.6 and A.7 were evaluated by dividing the ionosphere into layers of constant properties and summing the effects of the individual layers. Near the point of reflection the ionosphere was subdivided into layers of 1 km thickness. The summation was terminated at the top of the layer in which

APPENDIX A

$\mu=0$ so that μ had a small but finite value for the last term. In this way the infinity of the integrand in A.7 was avoided. The error in virtual height ($h'=c\tau_g$) introduced by this technique should be no larger than a few km. This accuracy should be sufficient for a qualitative picture.

APPENDIX B

Upper Atmosphere Models for Venus and Mars

Venus

The electron density profiles for the day and night sides of Venus shown in Figure B.1 are representative of the results of the Mariner 5 occultation experiment[1,2]. The altitude scale on this figure is based on an assumed radius of 6080 km. There is some uncertainty as to the radius of the planet (the radar radius is 6050) but this will not affect the following calculations. The rapid increase in density seen on the day side near 500 km and the near constant density region (10^4 cm^{-3}) between 400 and 200 km are thought to result from the compression and heating of the upper ionosphere by the pressure of the solar wind. The peak daytime electron density (10^6 cm^{-3} at 110 km) is similar to that on earth, however the scale heights (13 km for Venus just above the peak; ∿100 km for for earth) and the altitudes to the peak (110 km for Venus, 300 km for earth) are quite different (see also Figure B.2). The small scale height for Venus is probably indicative of of a cool ionosphere (∿300°K) compared to that on earth (∿10^3°K).

The maximum night density is 10^4 cm^{-3} and the altitude of the peak and the scale height above the peak are similar to those found on the day side. On the night side a near constant density region (10^3 cm^{-3}) extends from 200 to nearly 4000 km. At this point the density falls off rapidly to interplanetary values (∿5 cm^{-3}).

Since the ratio of the collision frequency to the wave frequency is small over most of the topside ionosphere, the real part of the index of refraction depends only on the electron density and the above data is adequate for the determination of the group delay (Equation A.4 and A.7). In order to calculate the collision frequency and the collisional absorption one must know also the electron temperature and the neutral density (A.2, A.3). The neutral density, composition, and temperature are fairly well known below 50 km[2], which is well below the ionospheric peak.

APPENDIX B

The neutral density and temperature at ionospheric heights can be inferred, however, if one makes certain assumptions as to the nature of the ionospheric layer. In this work the ions, electrons and neutrals will be assumed to be at the same temperature, a condition which is not true in the earth's ionosphere.

There are two general types of ionospheric layers, the Chapman, or photoequilibrium layer and the Bradbury, or diffusive equilibrium layer. In the Chapman-type layer the maximum electron density and the maximum production rate of ions occur at an altitude where the optical path for the ionizing radiation is equal to unity, that is, where the intensity of the solar ionizing radiation is reduced by e^{-1}. For earth the E and F_1 layers are of the Chapman type and they occur at neutral densities of the order of 10^{13} cm^{-3} and 10^{11} cm^{-3}, respectively.

In a Bradbury (F_2 layer on earth) a decrease in the recombination coefficient for ions and electrons coupled with plasma diffusion losses gives rise to a peak in the electron density profile which is above the altitude of the peak production rate of electrons. The neutral density at the F_2 peak on earth is of the order of 10^9 cm^{-3}.

The neutral density and temperature profiles for two daytime models for Venus are given in Figure B.3[2]. These two models represent an E-type layer with a neutral density of 10^{12} cm^{-3} at the ionospheric peak (110 km) and an F_1 layer with a neutral dnesity of 10^{11} cm^{-3} at 110 km. The higher temperatures in the E model are required in order to produce the higher neutral densities at the ionospheric peak.

The lack of atomic oxygen as determined by the ultraviolet experiment of Mariner 5 seems to rule out a Bradbury (F_2) type layer with the diffusive equilibrium of O^+ above the peak[2]. The positive ion near the peak is thought to be CO^+_2. This identification of the positive ion coupled with the measured scale height ($H=K(T_e+T_i)/M_i g$) leads to a temperature of about 300 °K just above the electron peak. The collision frequencies for the E and F_1 models are quite similar and are shown in the left hand portion of Figure B.1. In the F_1 model the collision frequency is dominated

APPENDIX B

by the electron-ion collision term above 120 km and by the electron-neutral term below this altitude. For the E model the electron-ion term dominates above 160 km and the rapid increase in collision frequency below this altitude is due to the contribution from electron-neutral collisions. The somewhat lower collision frequencies above 150 km for the E layer result from the higher temperatures in this model.

On the night side above 190 km the collision frequency is determined solely by electron-ion collisions and the values are lower than the two day side models because the (ion) densities are lower. Below 160 km the electron-neutral collisions dominate. The neutral densities in the night model were taken to be halfway between those of the E and F_1 models. The collision frequency for the earth model is given in Figure B.2 for comparison. Here the collision frequency is determined by electron-ion collisions over all the ranges shown.

Mars

The day side electron density profile for Mars is given in Figure B.4. That portion of the curve below 250 km was measured by the S-band (2300 MHz) occultation experiment of Mariner 4[3]. The solid curve above 250 km is an extrapolation with the observed scale height of 25 km. The dashed curve represents in an approximate fashion a model in which the upper ionosphere is compressed, as is the case for Venus. The S-band frequency experiment showed no effects attributable to a night side ionosphere and the densities must be less than 10^3 cm^{-3}.

Two models for the neutral density and temperature in the upper atmosphere are presented in Figure B.5. The model due to Fjeldbo et al.[7] is based on the photodissociation of CO_2 into CO and O and the diffusive equilibrium of these gases such that O is the predominant neutral constituent above 90 km. This model represents a Bradbury or F_2 ionospheric layer and has a neutral density of 10^9 cm^{-3} at the altitude of the electron density peak (125 km). The positive ion in the main ionospheric layer is thought to be O^+.

APPENDIX B

The second model is after Chamberlain and McElroy[8] and it represents an E-type layer in that the neutral density at the ionospheric peak is of the order of 10^{13} cm^{-3}. It differs from the above model in that the photodissociation products of CO_2 are mixed uniformly throughout the upper atmosphere.

The collision frequency profiles are given in Figure B.6 for these two models. The F_2 model has the electron-ion collision term dominant above 90 km and the electron-neutral term dominant below. In the E layer model the two terms are comparable above 150 km and the electron-neutral term is dominant below this altitude.

APPENDIX C

Calculation of Collisional Absorption and Group Delay in the Topside Ionospheres of Venus and Mars

The integrals in Equations A.6 and A.7 for the collisional absorption and the group time delay were numerically evaluated by constructing layered models of constant properties and summing the effects of each layer. The layer thickness was 50 km between 500 and 200 km and 10 km below this altitude. Near the point of reflection an interpolation routine further divided the region into layers of 1 km thickness.

The collisional absorption is expressed in db

where

$$db = 20 \log (R)$$

$$R = e^{-k_o \int_S \chi ds} \qquad C.1$$

The path S is taken from the altitude of the satellite (500 km for Venus and Mars, 1000 km for earth) to the point of reflection in the ionosphere.

The group delay is expressed in terms of the virtual range (h') which is the distance a wave propagating at the speed of light would travel in an equivalent time.

$$h' = c\tau_g = \int_S \frac{ds}{\mu}$$

The virtual range curve as a function of frequency is called an ionogram. Since the waves are reflected from an altitude where the wave frequency is equal to the plasma frequency and since the plasma frequency is proportional to the square root of the electron density, then the ionogram represents an electron density profile in terms of the virtual range.

APPENDIX C

Techniques have been developed for converting the virtual range data into electron density profiles as a function of true range or altitude.

Venus

Figure C.1 contains curves of the collisional absorption as a function of the frequency of the sounding wave for the earth and Venus models of Appendix B. For the earth the absorption varies between -1 and -5 db and is largest for the highest frequencies where the path lengths are longest. In the dayside ionosphere of Venus the attenuation in the frequency range between 1 and 6 MHz is of of the order of -2 db; above 6 MHz the attenuation increases rapidly to -13 db at 9 MHz. The rapid increase in absorption above 6 MHz is due to the fact that these waves reflect below 140 km which is a region of rapidly increasing collision frequency. The absorption in the F_1 model is slightly greater than that in the E model except at the very highest frequencies near 9 MHz. At these frequencies the waves in the E model penetrate a region near the ionospheric peak where the collision frequency exceeds that in the F_1 model.

On the night side the absorption is of the order of -.1 db for frequencies between .2 and .7 MHz. Above .8 MHz the absorption rises rapidly from -.3 db to -5 db at .9 MHz.

The virtual range (h') or ionogram and the true range curves for the Venus day and night models are presented in Figure C.2. The large differences in the true and virtual ranges for frequencies between 1 and 3 MHz on the day side and between .3 and .5 MHz on the night side result from the ledge of near constant density above 200 km altitude. Those sounding waves with frequencies just above the ledge plasma frequency are traveling large distances in a medium where their frequency is close to the plasma frequency and hence the group velocity is low. The low group velocity leads to large virtual ranges. As the wave frequency increases above the ledge plasma frequency the group velocity in the ledge region increases and the difference between the virtual and true range decreases. As can be seen from these curves the presence of the ledge obscures the effects due to the lowering of the reflection point as the frequency increases. Accurate measurements in the small scale height region just above the peak would require a virtual range resolution of at least

3 km (time resolution of 10 μsec), which is about an order of magnitude better resolution than is used on typical earth orbiting topside sounders.

Mars

The collisional absorption curves for the Martian models are presented in Figure C.3. For frequencies between .6 and 2 MHz the results for both models (F_2 and E) show an increase in attenuation from -.1 db to -2 db. Above 2 MHz the attenuation increases to a maximum of -8 db at 2.85 MHz for for the F_2 model, while the E model, due to its large collisional frequencies near the peak, increases to a maximum of -70 db. The very large collisional absorption associated with the E layer model would present severe problems for the design of a topside sounder. The Martian E model losses are considerably larger than those of the Venus E model, which has similar electron-neutral collision frequencies near the peak, because of the lower plasma frequencies (lower electron densities). This results from the fact that for Mars the ratio $Z=\nu/\omega$, which enters into the calculation of the losses (Equation A.1, A.5, A.6), is larger since the frequency ($\omega=\omega_p$ at reflection) is smaller.

The virtual range (ionogram) and true range curves for the electron density profiles of the Martian ionosphere are given in Figure C.4. The solid curves for the true and virtual range are for the model with a constant scale height of 25 km above the peak. In this case the virtual height curve is similar in form to the true range curve and has a scale height only slightly greater than the true scale height of 25 km. The dashed true range curve below .75 MHz is for the model with a ledge or rapid increase in scale height. As is the case for Venus the corresponding dashed virtual height curve differs considerably in form from the true height curve. Once again the small scale height above the peak necessitates a better range (or time) resolution than is commonly found on earth topside sounders.

In the models presented in Appendix B, certain assumptions were made about the nature of the layer in order to extrapolate the neutral density from the lower altitudes, where it is measured, to the altitude of the ionospheric peak and above. In the F_2 and F_1 models the absorption at the peak and above is a result of the electron-ion collisions so that

in these models, the exact knowledge of the neutral density profile is not crucial to the calculations. However in the E layer models the absorption near the peak results from electron-neutral collisions and here the maximum attenuation, which occurs at the highest frequencies, will depend strongly on the neutral density profile.

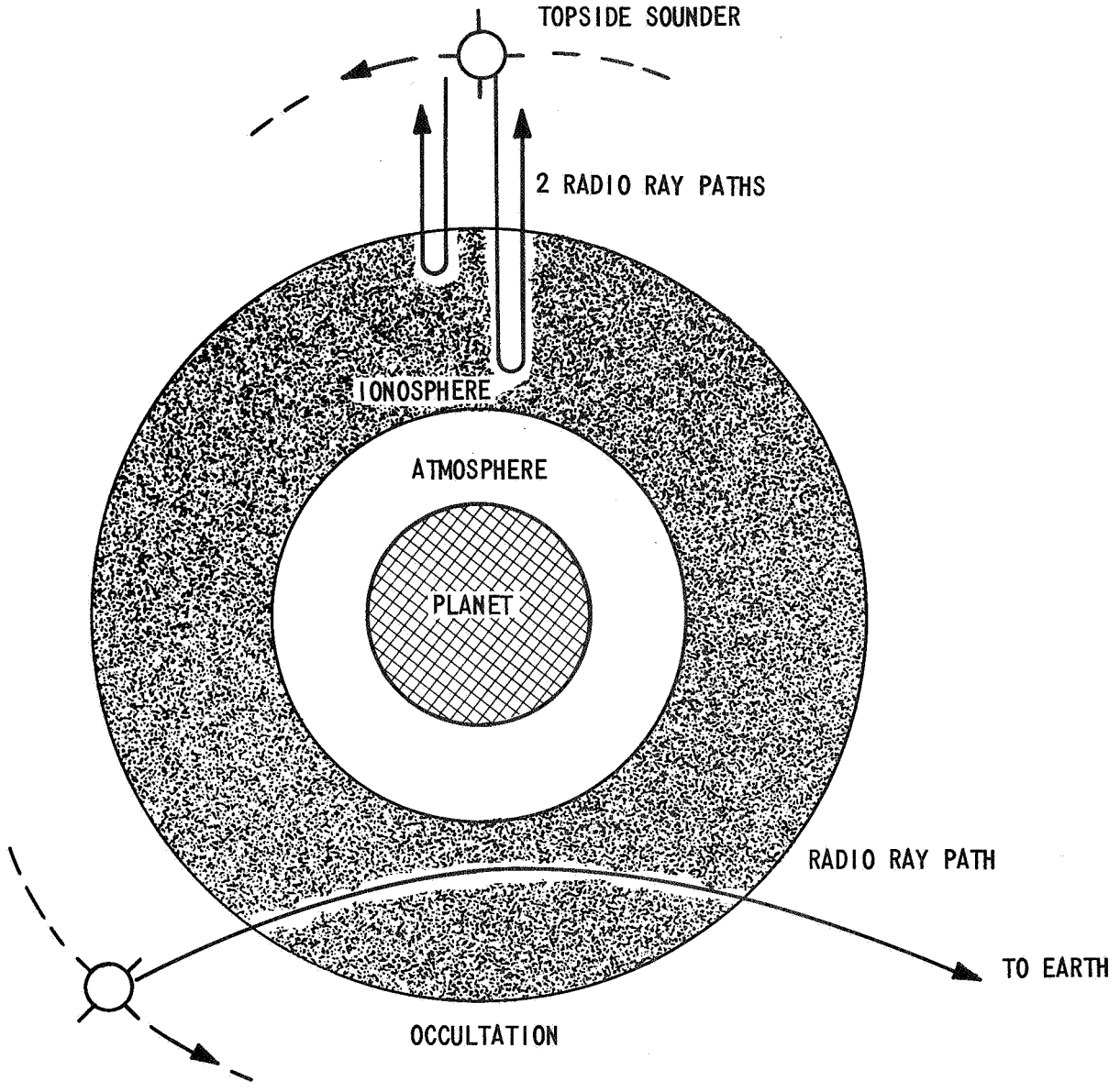

FIGURE 1. GEOMETRY OF TOPSIDE SOUNDER AND OCCULTATION EXPERIMENTS.

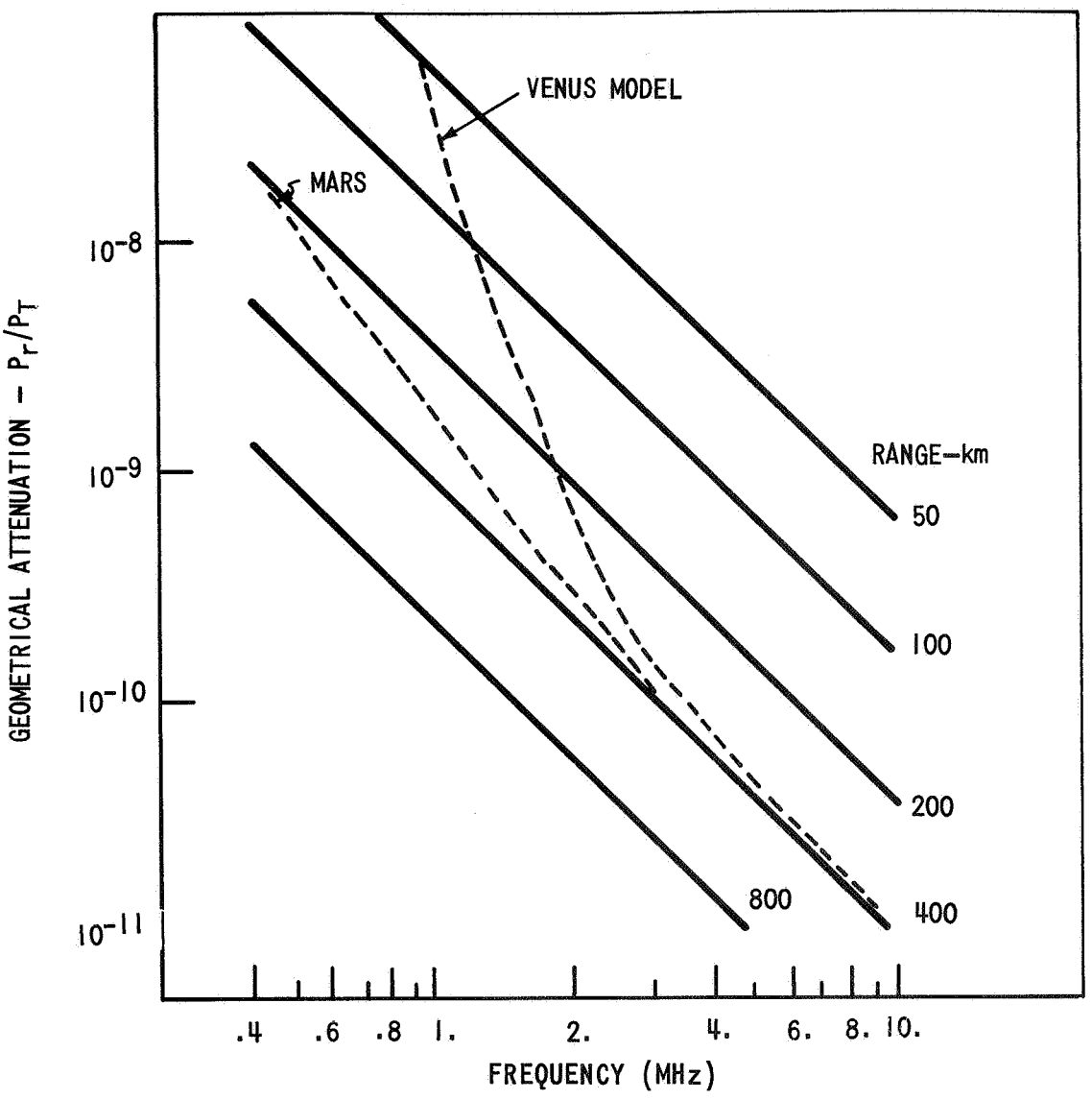

FIGURE 2. GEOMETRICAL ATTENUATION AS A FUNCTION OF FREQUENCY AND RANGE

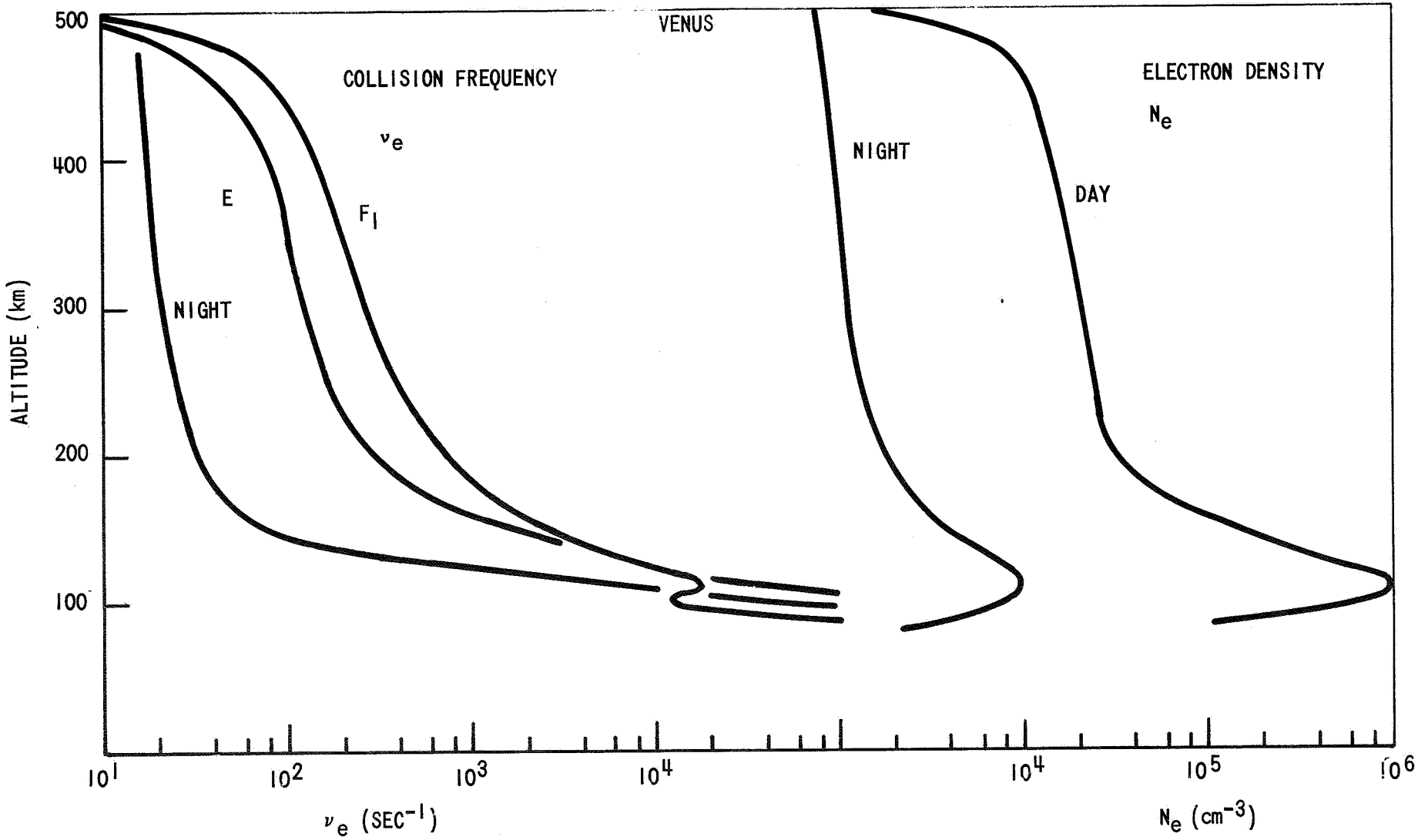

FIGURE B.1. VENUS, ELECTRON DENSITY AND COLLISION FREQUENCY PROFILES

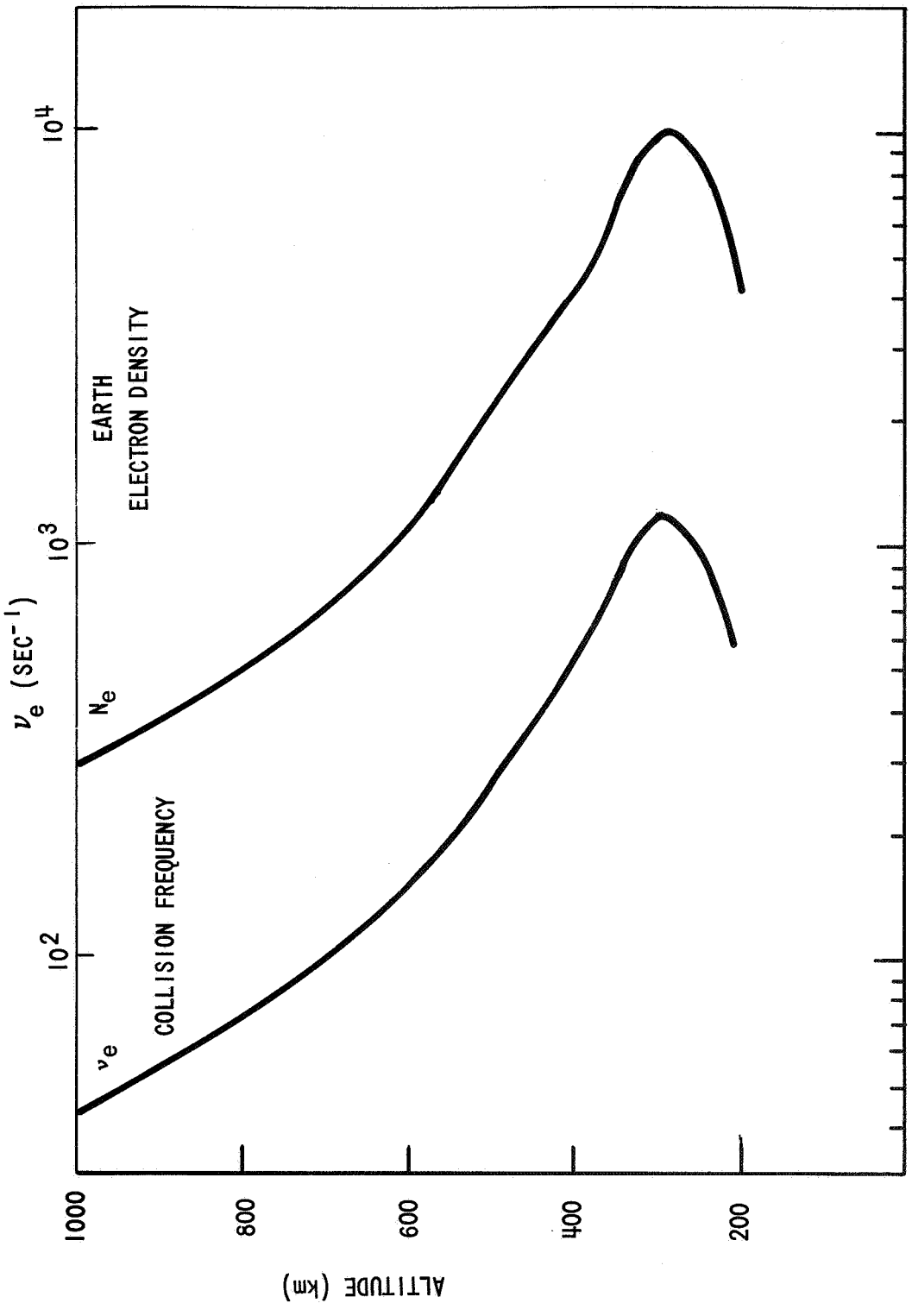

FIGURE B.2. EARTH, ELECTRON DENSITY AND COLLISION FREQUENCY PROFILES

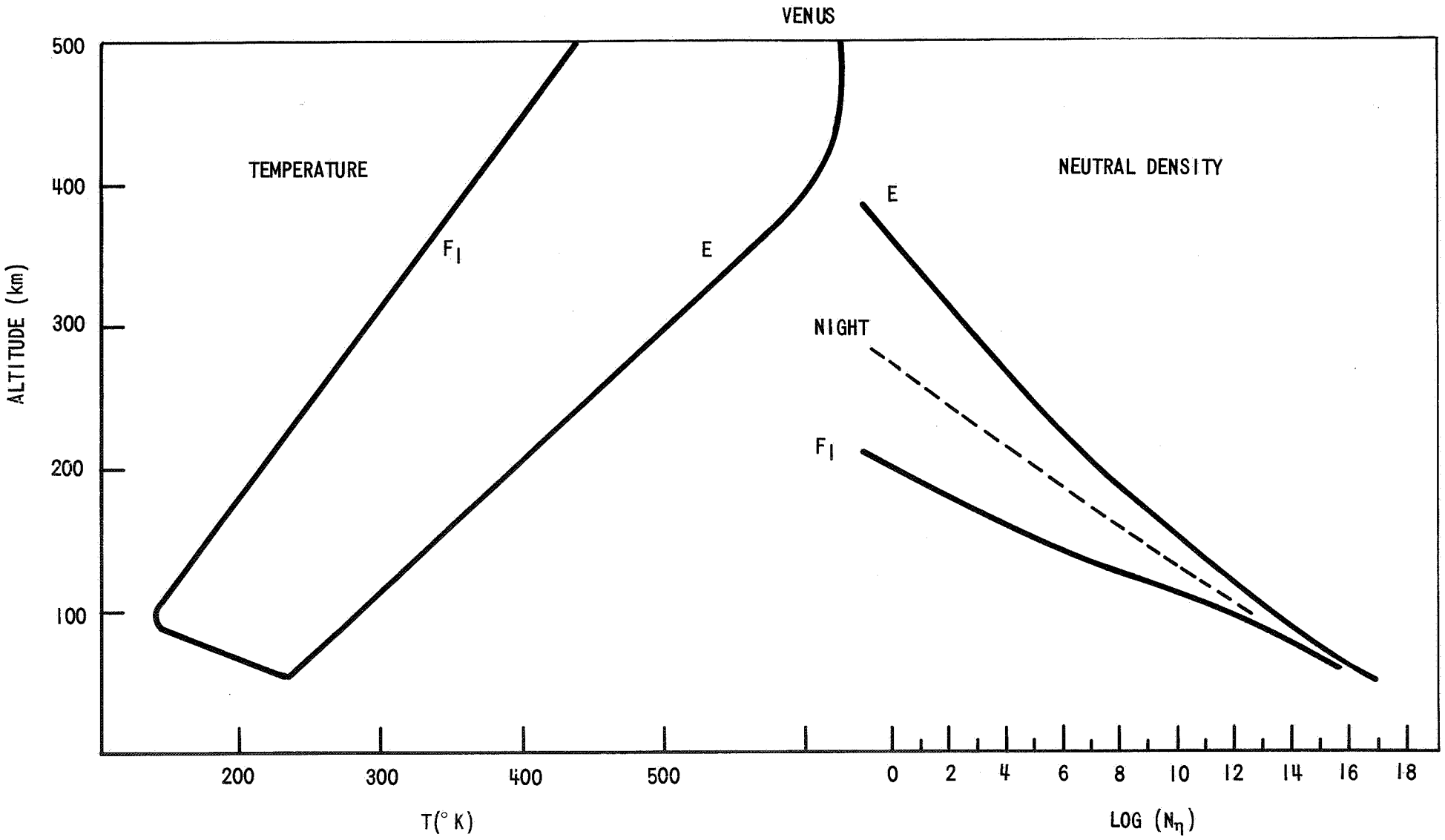

FIGURE B.3. VENUS, TEMPERATURE AND NEUTRAL DENSITY PROFILES

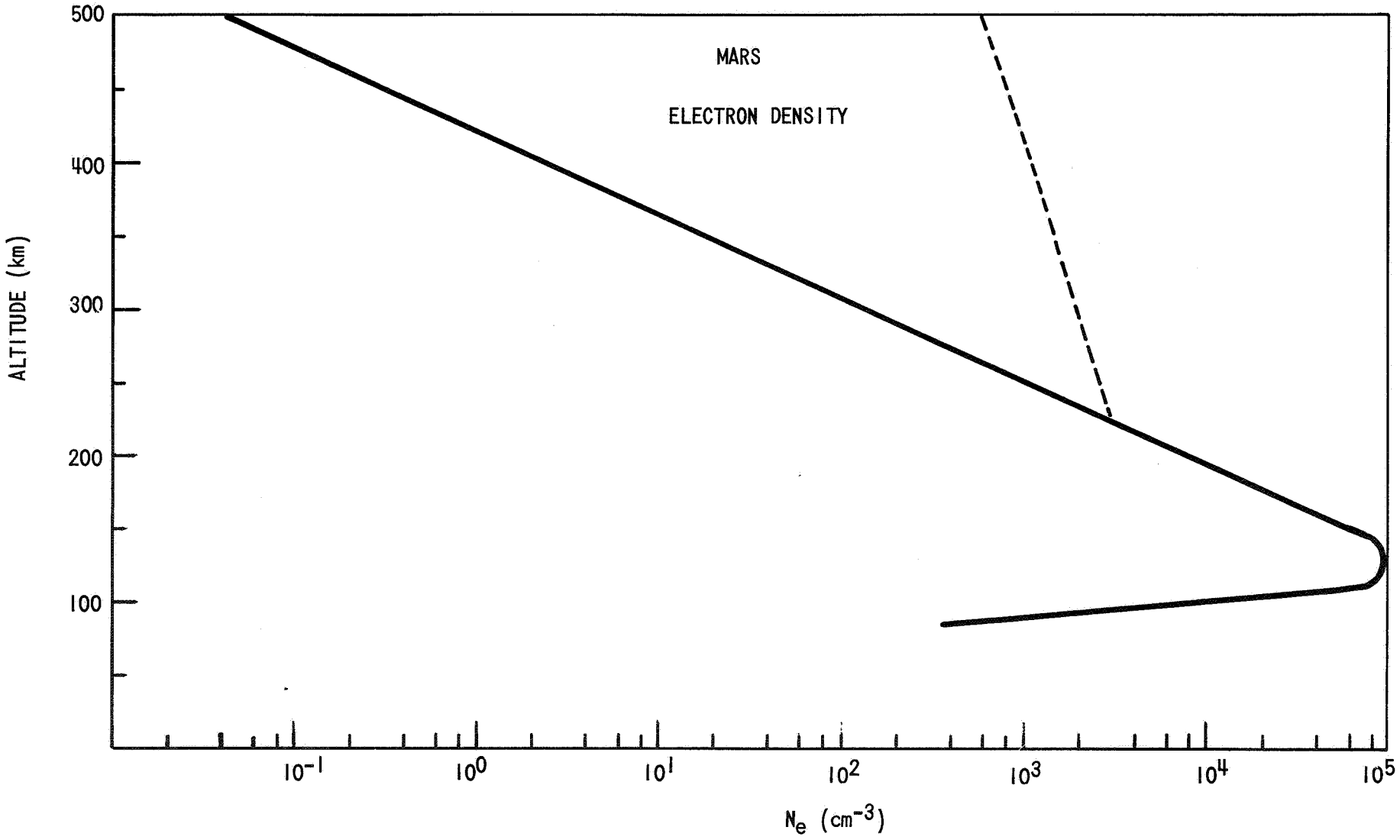

FIGURE B.4. MARS, ELECTRON DENSITY PROFILE

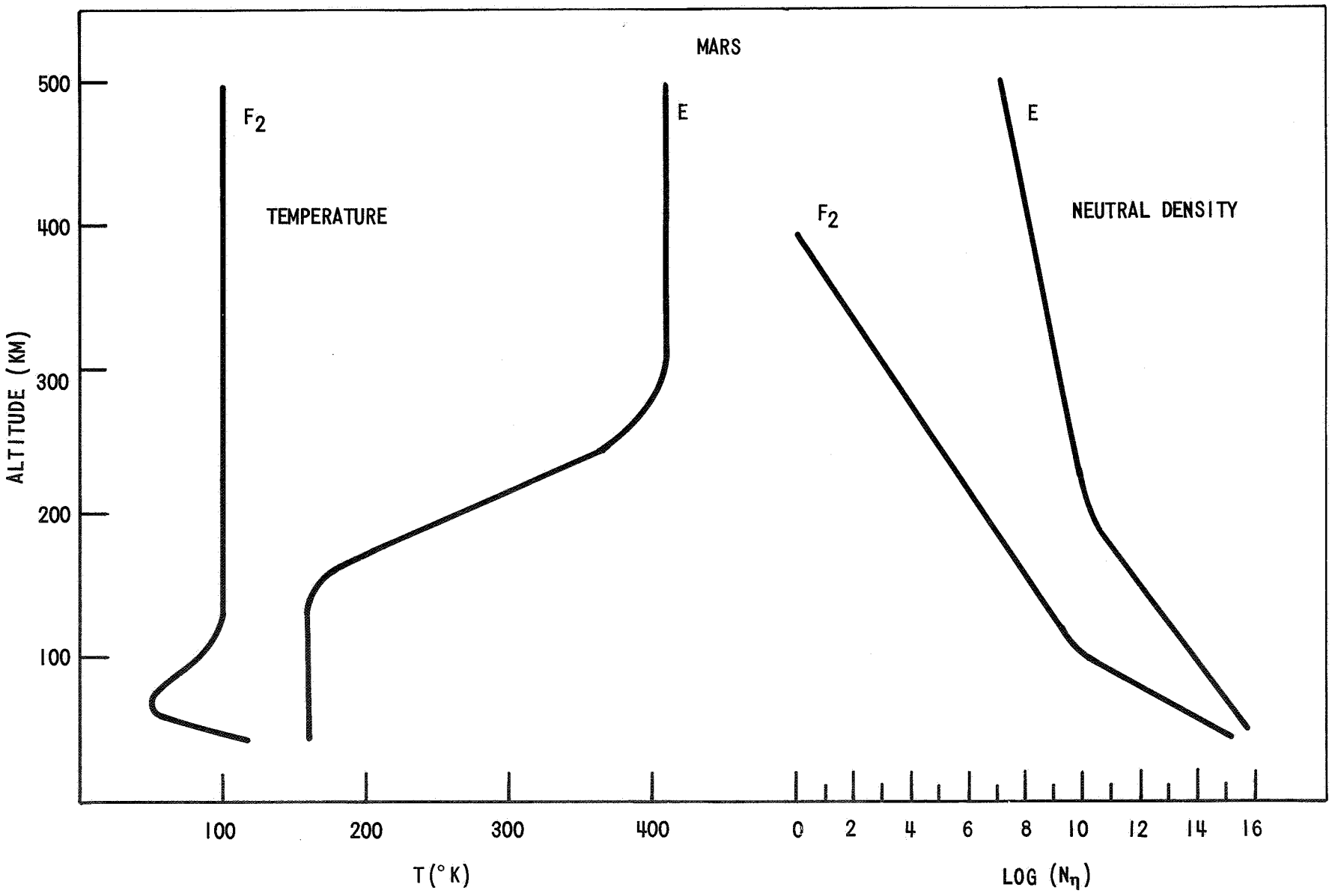

FIGURE B.5. MARS, TEMPERATURE AND NEUTRAL DENSITY PROFILES

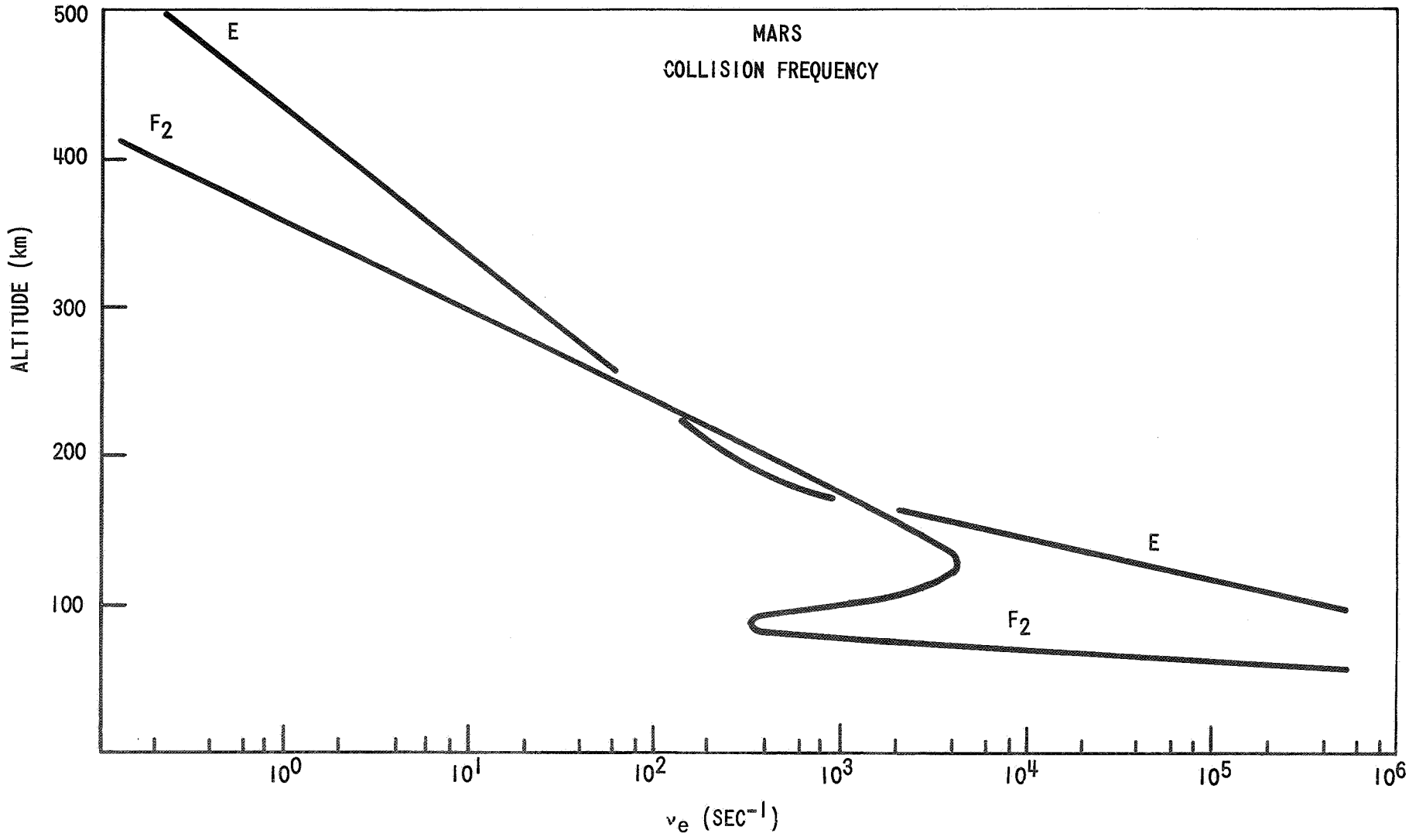

FIGURE B.6. MARS, COLLISION FREQUENCY PROFILE

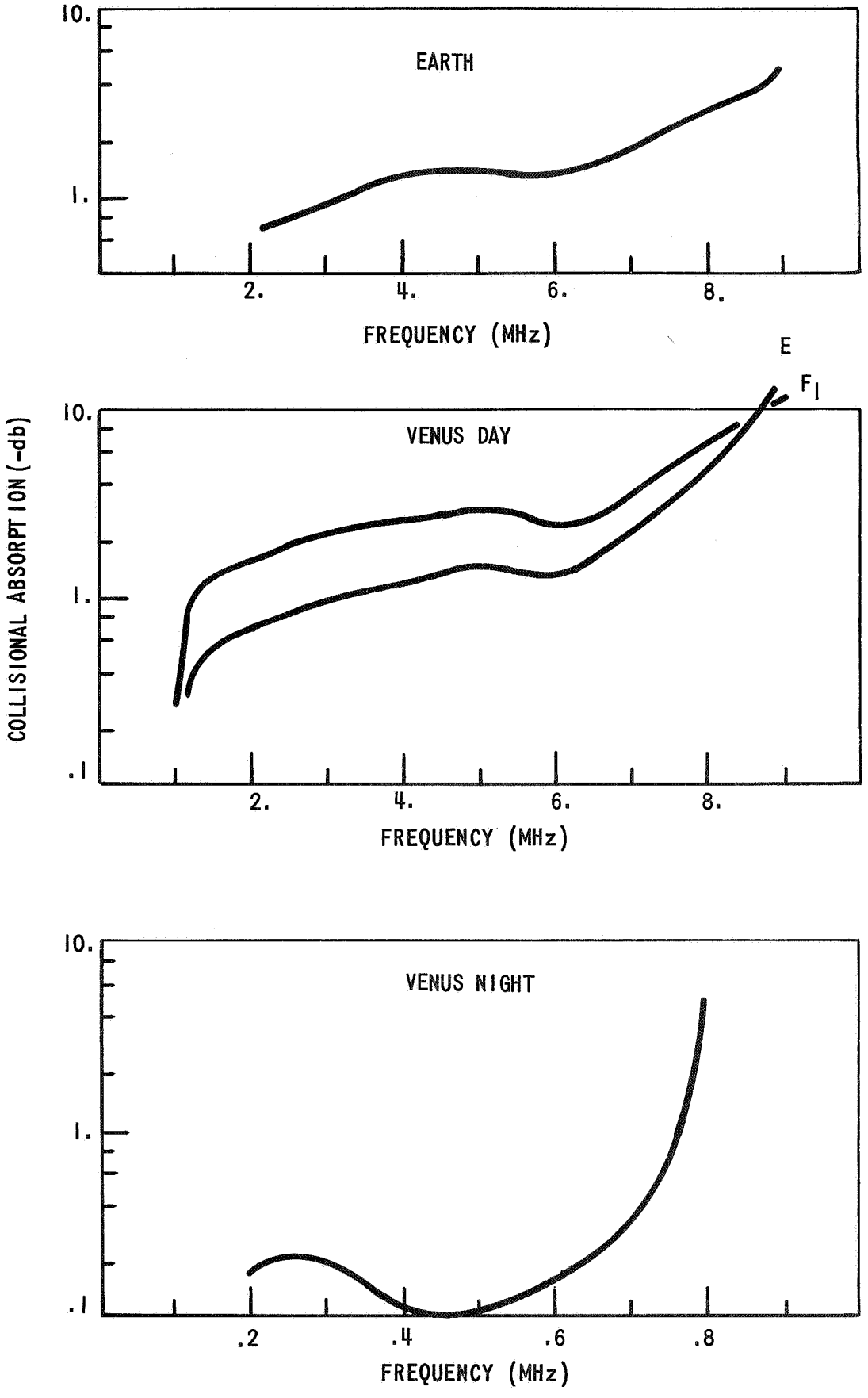

FIGURE C.1. ELECTRON COLLISIONAL ABSORPTION, EARTH AND VENUS

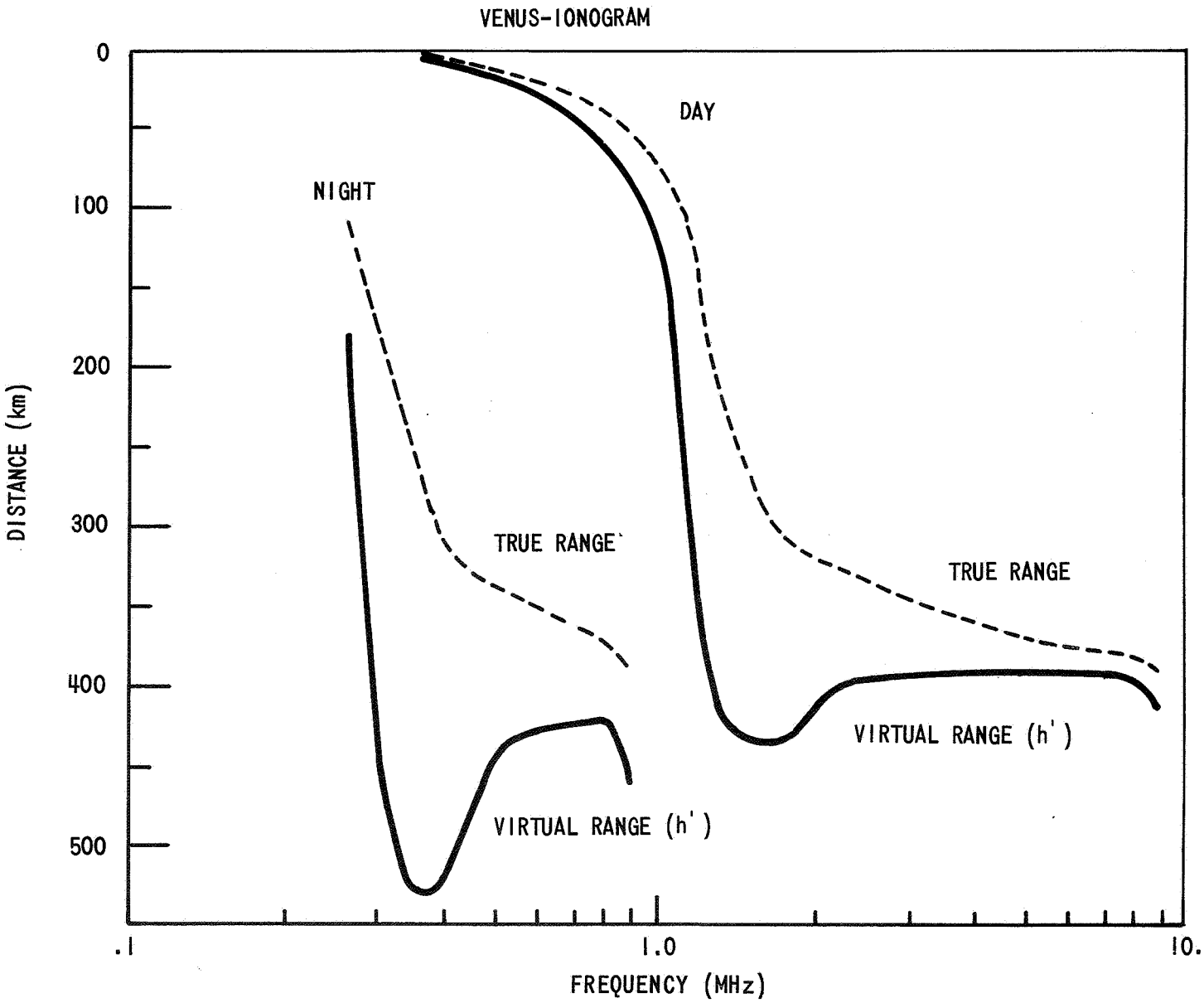

FIGURE C.2. VENUS IONOGRAMS

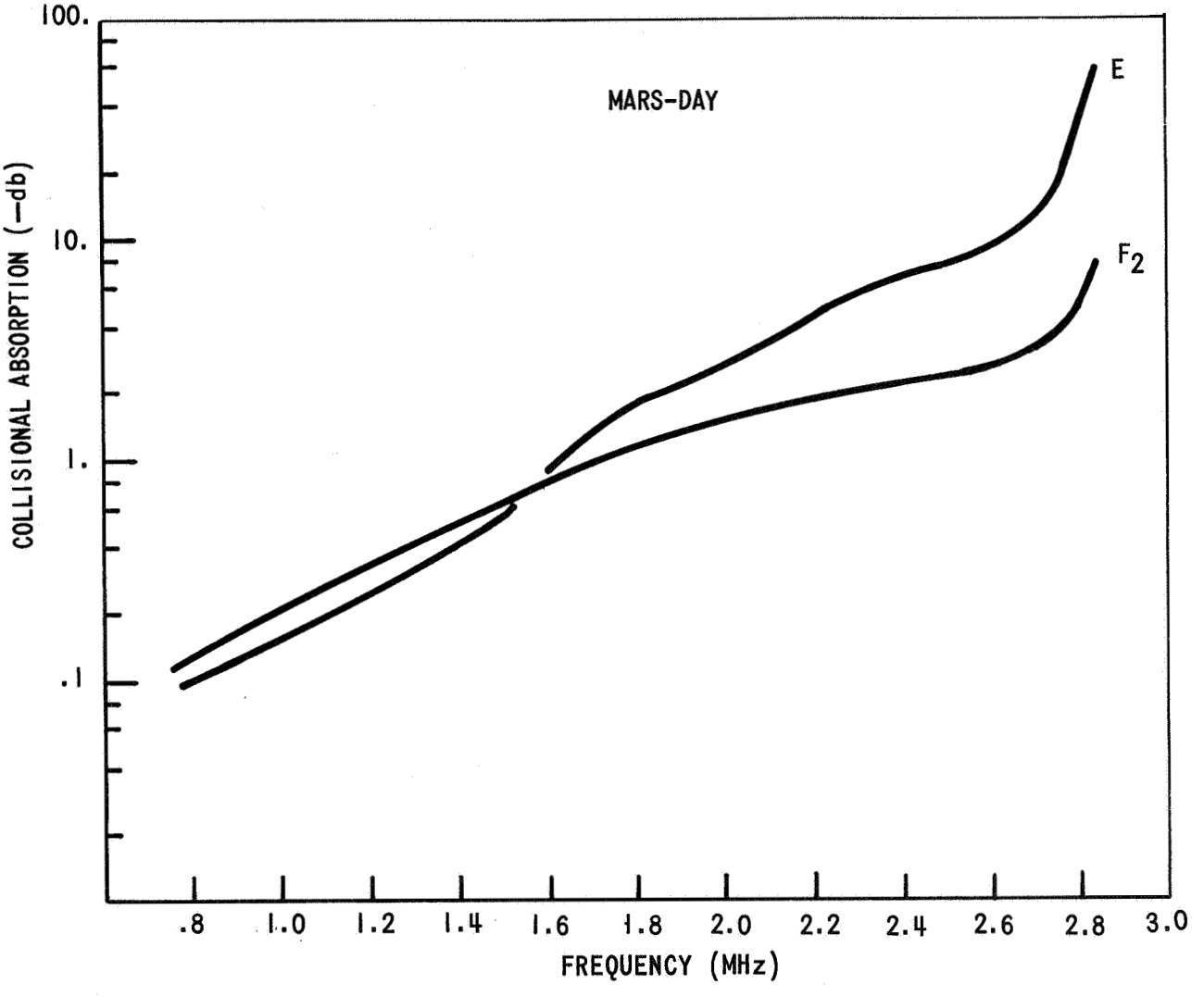

FIGURE C.3. MARS, ELECTRON COLLISIONAL ABSORPTION

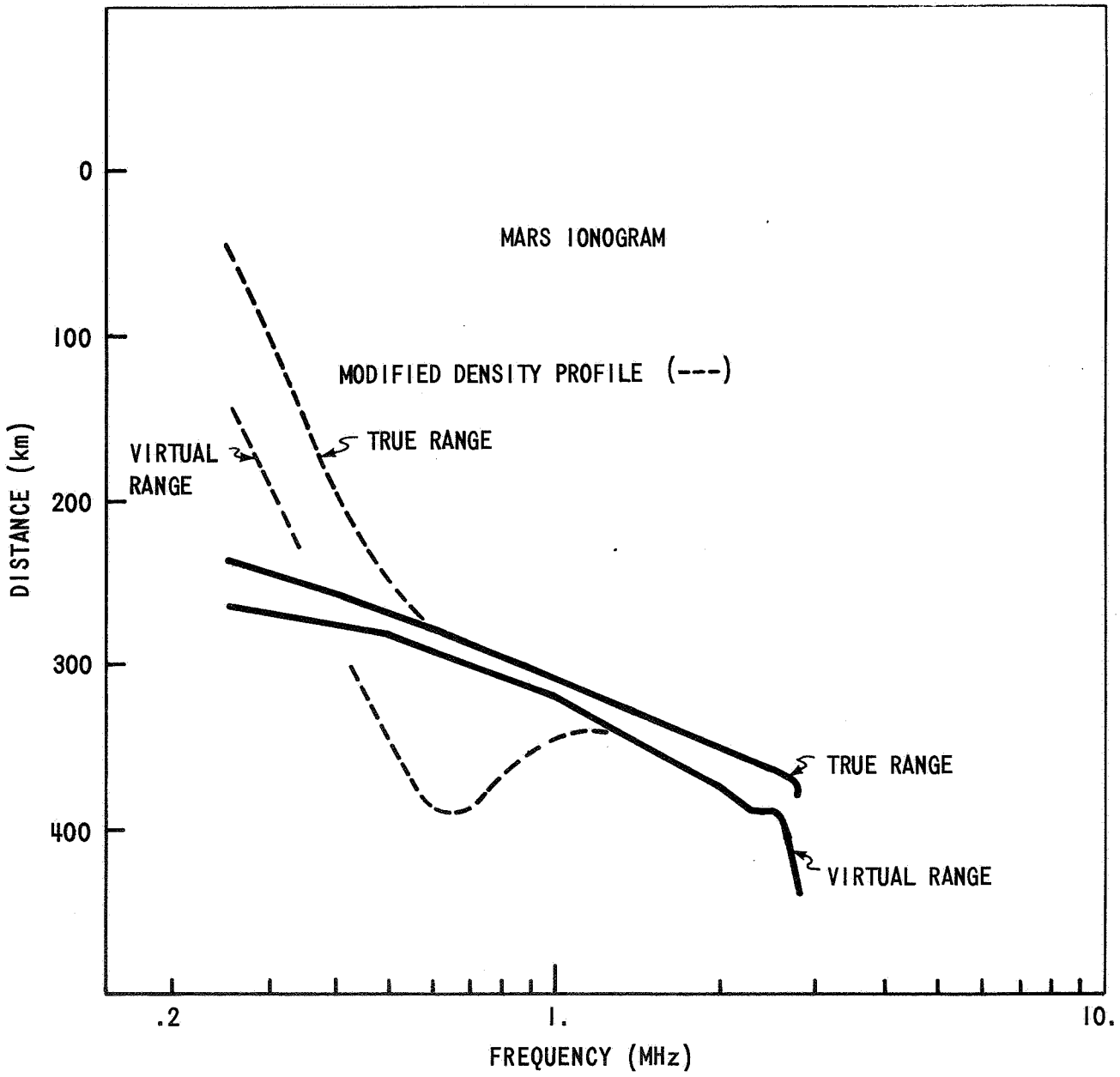

FIGURE C.4. MARS IONOGRAMS

Distribution List

NASA Headquarters
Messrs. W. O. Armstrong/MTX
N. W. Cunningham/SL
F. P. Dixon/MTY
S. E. Dwornik/SL
R. F. Fellows/SL
E. W. Glahn/SL
E. W. Hall/MTG
D. P. Hearth/SL
T. A. Keegan/MA-2
R. S. Kraemer/SL
D. R. Lord/MTD
B. G. Noblitt/MTY
D. G. Rae/SL
G. A. Reiff/SL
E. R. Schmerling/SG
A. D. Schnyer/MTV
J. W. Wild/MTE

Ames Research Center
I. G. Poppoff/SSA
L. Roberts/M (2)
C. P. Sonett/SS
P. R. Swan/MS

Goddard Space Flight Center
A. C. Aikin, Jr./615
S. J. Bauer/615
E. D. Nelson/615
N. F. Ness/612
T. G. Northorp/640
L. S. Walter/644

Jet Propulsion Laboratory
R. G. Brereton/161
D. L. Cain/311
A. Kliore/311
G. S. Levy/333
R. V. Meghreblian/32
C. W. Snyder/251

M.I.T. Lincoln Laboratory
J. V. Evans

Stanford University,
Center for Radio
Astronomy
Messrs. R. B. Dyce
V. R. Eshleman
G. Fjeldbo

Bellcomm, Inc.
F. G. Allen
G. M. Anderson
A. P. Boysen, Jr.
D. A. Chisholm
C. L. Davis
D. A. DeGraff
J. P. Downs
R. E. Gradle
D. R. Hagner
P. L. Havenstein
N. W. Hinners
B. T. Howard
D. B. James
J. Kranton
H. S. London
K. E. Martersteck
R. K. McFarland
J. Z. Menard
G. T. Orrok
T. L. Powers
I. M. Ross
F. N. Schmidt
W. B. Thompson
C. C. Tiffany
J. W. Timko
J. M. Tschirgi
R. L. Wagner
J. E. Waldo
All members, Division 101
Central Files
Department 1023
Library